Numerical modelling of island and capture zone size distributions in thin film growth

by

Antonis Neochoritis

August 2005

Abstract

The Mulheran and Robbie theory of island and capture zone size distribution in thin film growth has been studied using an equation which describes both the island growth inside the capture zones and the fragmentation which occurs at the island nucleation rate. We have numerically approximated the governing differential equation and a boundary condition equation, which have been solved simultaneously using an integration method in two steps, a Semi – Lagrange step and a Runge – Kutta second order step. A FORTRAN 90 programme was constructed to investigate the model, which generates profiles from a given initial data function.

Acknowledgements

I would like to thank my supervisors, Professor Mike Baines and Dr. Paul Mulheran, for their support throughout this project. My gratitude is also due to the head of the Mathematics department, Dr. Peter Sweby, for encouraging me to attend this MSc course, and to the head of the Physics department, Professor John Blackman, for his support and helpful discussions, especially during the last part of this project. Last but not least, to express my appreciation to my friend Christiana Pliaka for checking and advising on the structure and accuracy of the English text.

Declaration

I confirm that this is my own work, and the use of all material from other sources has been properly and fully acknowledged.

To Professor Mike Baines, without whose delightful sense of humour, extreme patience and empathy towards mathematical concepts, this work might well have become just another academic exercise.

Contents

List of figures

Chapter 1.

Introduction

Nanotechnology is the science and engineering of the materials on the scales of atoms[1]. A nanometre (nm) is one-billionth of the metre (10^{-9} m) , or the length of ten times the diameter of hydrogen atom. Advocates of this new multidisciplinary area of research promise strong polymer constructions, clean energy, and nanorobotic devices which repair damage and infections in human cells.

The aim of this project is not only to describe the theory of the island and capture zone size distribution, but also to implement a numerical technique which can be used to find the approximate solution of the differential equations that express the model.

1.1 A brief history of Nanotechnology

The idea of nanotechnology materialized in 1959, when Richard Feynman gave a lecture entitled *" There is plenty of room at the bottom"* . Feynman proposed the idea of developing things on the atomic scale, just as nature does [1]. The term nanotechnology was coined by Professor Norio Taniguichi in 1974, and in 1986 the term was defined by K. Eric Drexler in his book, *" Engines of Creation : The coming era of Nanotechnology"* [2].

Experimental nanotechnology started after the invention of the scanning tunnelling microscope (STM) by IBM researchers in Zurich , Switzerland, in 1981 , which made it possible to observe the atomic world [1].

On such small scales the properties of materials change in counterintuitive ways; for example, tiny particles of gold melt between 600^0C - 800^0C, while a large nugget melts at 1064^0C [3]. This happens because of two main reasons:

(a) the ratio of surface of the material to its volume increases, and atoms on these surfaces are more active than those at the centre of the material,

(b) at small scales, matter follows the laws of quantum mechanics and is also partially affected by molecular Van der Waals forces. According to Heisenberg's uncertainty principle, we cannot know the exact position and momentum of a particle, and if we restrict an electron by reducing the dimensions of a metal (to which the electron belongs), its energy increases [4] .

Nanotechnology affects a wide variety of industries because it can improve the existing identities of materials or create new structures by combining synthetic and natural components.

1.2 Nanostructures and applications of nanotechnology

Nanotubes. In 1985, chemists discover how we can create a soccer ball – shaped molecule of 60 carbon atoms (buckminsterfullerene or C_{60}) and in 1991, a researcher at the NEC corporation discovered a new form of carbon known as carbon nanotubes, which is much stronger than graphite and six times lighter than steel. A nanotube is like a very strong sheet of graphite rolled into a cylinder, and can behave either as a metal or as a semiconductor, depending on how the carbon hexagons are arranged [5] . This unique material has been made into fibres, maybe the world's strongest polymer, and can be used in batteries, computer chips and sensors, or in next – generation spacecrafts.

Quantum dots are nanocrystals measuring only a few nanometres. Because of their size, approximately the same as that of a protein molecule, they are used as probes in living cells and help researchers in medical diagnostics and gene expression analysis [6] .NASA researchers developed a synthesis of quantum dots of $CuInS_2$ and CdSe useful in solar cells, that create an intermediate band which allows the harvesting of large portion of the solar spectrum [7] .

Environmental Applications . Nanotechnology provides many environmental benefits. Nanoscale filters can improve water purification systems, neutralise toxic materials and clean up heavy metals and chemical pollution. By using nanotechnology techniques, developing countries can grow crops in fields with high levels of salt or low levels of water. Similarly, by using nanotechnology, Thailand physicists have rearranged rice DNA to develop a new rice plant which produces a better quality crops which is insensitive to sunlight [8] , [9] .

Nanomedicine is the application of nanotechnology in medical diagnostics and research [10]. By using nanopolymer capsules, we can deliver precise doses of medicine through the patient's bloodstream directly to the affected area and nanorobots can identify cancer affected cells by using molecular markers [10]. Medical nanorobots, usually 0.5 – 3 micrometer in size, allow instant pathogen diagnosis or replacement of chromosomes and individual surgery in vivo [11] . Nanorobots could also deliver chemotherapy direct to tumours, minimizing the side effects to surrounding tissue.

1.3 Potential risks

Nanoparticles are likely to be more toxic and their chemical and biochemical properties will be different from those of bulk solids. It is already known that some nanoparticles are harmful to mice and fish [6]. The worst scenario is the **grey –goo** idea . This term, which was coined by Eric Drexler, describes the hypothetical end of the world because nanorobots might self-replicate uncontrollably and turn the Earth into grey goo [12] . So a moratorium might be needed in order to release nanoparticles into the environment when it is clear that they are safe for the environment and human health [13].Therefore it is important to study in depth and model this well promising scientific area.

1.4 Plan of Dissertation

In chapter 2 we state some definitions appropriate for understanding the model. In chapter 3 there is the description of the model and in the next chapter we analyze the numerical techniques used. The method of solution is explained in

chapter 5 and in the following two chapters there are numerical results and general discussion.

Chapter 2

Definitions

Atoms aggregate in order to gain binding energy and become more stable . This theory derives its origin from a 1921 study by Polish physicist Marian von Smoluchowski, who propounded the aggregation theory to describe the microscopic diffusion process [14].

A Nanoparticle is a group of atoms, or just one atom, depending on the material. The process by which an atom or a Nanoparticle forms bonds with atoms on the surface of the nanomaterial and sticks with them is defined as a **deposition** [15] .

An island is a group of nanoparticles. In nanotechnology the size of an island is important because it affects the usefulness of the nanomaterial. The critical size i of an island expresses the number of the monomers that it has absorbed . The parameter i depends on the material's temperature, it increases as the temperature increases [16] , and it is an integer . When an island absorbs i+1 monomers, it becomes stable. Islands are represented by small circles which are centred on their nucleation site , not only for computation reasons but also because circles reflect the underlying grid symmetry .

The capture zone of an island (see figure **2.1**) is the area of the substrate where monomers are more able to diffuse into this particular island than to any other island in the substrate [16] (page 10261). The geometrical approximation of a capture zone is a Voronoi polygon, which is defined as the set of points :

$$V_i = \{ \tilde{X} : \| \tilde{X} - \tilde{X}_i \| < \| \tilde{X} - \tilde{X}_j \| \quad \forall \; i \neq j \} \quad .$$

In practice the boundary of each polygon is made of segments of the perpendicular bisectors to the lines which joins the node to every other node (figure **2.2**).

When an island absorbs monomers, the Voronoi polygon network is updated .

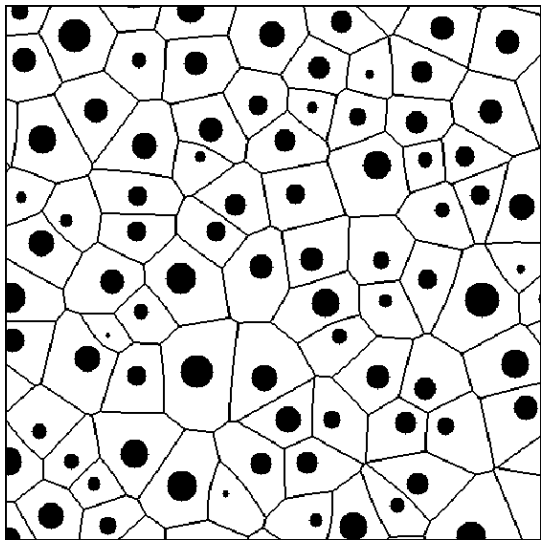

figure 2.1

A snapshot of islands and Voronoi polygons capture zones for island size i=1 (courtesy of P. Mulheran).

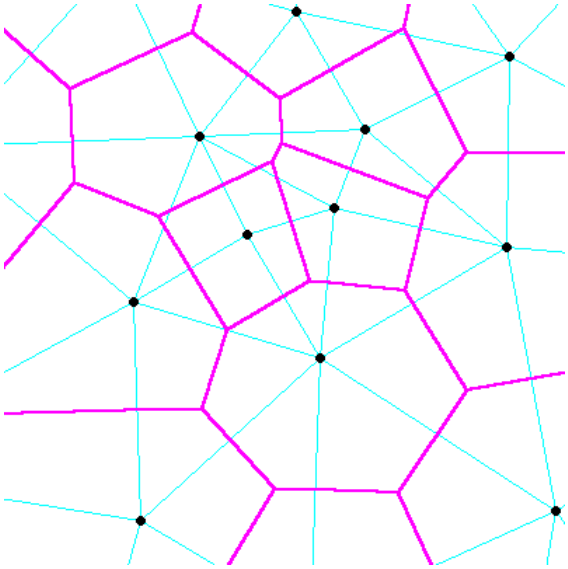

figure 2.2

Voronoi polygons

http://www.geodyssey.com/tutorial/tc06.html

Chapter 3

Model description

The paper *" Theory of the island and capture zone size distribution in thin film growth"* , by P. A. Mulheran and D. A. Robbie [17], studies the evolution of capture zones when new islands nucleate and reveals crescent nucleation when the critical island size is i = 0 . The model in the paper is based on four principles:

1. Islands grow consecutively at a rate analogous to their capture zone size .

2. Island nucleation occurs according to Mean – Field Theory . The main idea of this theory is that we can replace the interaction of a part of a field by the average of neighbour interactions .

3. Each nucleation that occurs divides the island's capture zone, taking a proportion λ in order to construct the new island's capture zone and leaving $1-\lambda$ to the existing island . This is a simplification of reality , where a new island constructs its capture zone by taking small parts of neighbouring island's capture zones and not just from one, but numerical simulations of the model show that there is little difference in the effect on the results.

4. The fragmentation probability in a capture zone , which has size a , is :

$$p(a) \approx a^{2i+2}$$

where i is the critical size of the island .

If we consider the joint distribution $f(a,s,t)\,da\,ds$ which represents the number of islands of sizes between s and $s+ds$ inside the capture zones of sizes between a and $a+da$ at time t. Then for island sizes greater than $s_0 = i+1$ the above rules are expressed by the equation:

$$\frac{d}{dt}\int_{s_1}^{s_2} f(a,s,t)ds = -\frac{Ra}{\Omega}[f(a,s_2,t) - f(a,s_1,t)]$$

$$+\frac{\dot{N}(t)a^{2i+2}}{m_{2i+2}(t)}[-\int_{s_1}^{s_2} f(a,s,t)ds + \frac{1}{(1-\lambda)^{2i+3}}\int_{s_1}^{s_2} f(\frac{a}{1-\lambda},s,t)ds] \quad \textbf{(3.1)}$$

$\forall$ s_1, s_2, which leads to the partial differential equation:

$$\frac{\partial}{\partial t} f(a,s,t) = -\frac{Ra}{\Omega}\frac{\partial f(a,s,t)}{\partial s} +$$

$$\dot{N}(t)\frac{a^{2i+2}}{m_{2i+2}(t)}[-f(a,s,t) + \frac{1}{(1-\lambda)^{2i+3}} f(\frac{a}{1-\lambda},s,t)] \quad \textbf{(3.2)}$$

for $t > t_0$, $s > s_0$, where R is the monomer deposition rate, Ω is the total area of the substrate and are constants, $N(t)$ is the island nucleation rate and

$$m_{2i+2}(t) = \int_{a_{\min}}^{a_{\max}}\int_{s_0}^{s_{\max}} a^{2i+2} f(a,s,t)dsda\,, \quad \textbf{(3.3)}$$

is the $2i+2$ moment of the distribution that normalises the fragmentation probability . It is this normalisation factor which couples together the equations for all a and s.

The term

$$-\frac{Ra}{\Omega}[f(a,s_2,t) - f(a,s_1,t)] \quad \text{of} \quad \textbf{(3.1)}$$

accounts for the island growth.

The term

$$\dot{N}(t)\frac{a^{2i+2}}{m_{2i+2}(t)}[-\int_{s_1}^{s_2} f(a,s,t)ds + \frac{1}{(1-\lambda)^{2i+3}}\int_{s_1}^{s_2} f(\frac{a}{1-\lambda},s,t)ds]$$

of (**3.1**) expresses the fragmentation of the capture zone, while the term

$$\frac{1}{(1-\lambda)^{2i+3}}$$

accounts for the fragmentation that occurs in capture zones of sizes between

$$\frac{a}{1-\lambda} \quad \text{and} \quad \frac{a+da}{1-\lambda} \ .$$

For the minimum island size $s = s_0$ the model equation corresponding to (**3.2**) is assumed to be:

$$\frac{\partial}{\partial t} f(a, s_0, t) = -\frac{Ra}{\Omega ds} f(a, s_0, t) + \dot{N}(t) \frac{a^{2i+2}}{m_{2i+2}(t)} \frac{1}{\lambda^{2i+3}} \sum_{s>s_0} f(\frac{a}{\lambda}, s, t) \quad \textbf{(3.4)}$$

at $t > t_0$, which expresses the fragmentation process that creates islands of size $s_0 = i+1$. The capture zone size in this particular case is finite and the term which expresses the island growth is a dimensionally correct estimate of the local behaviour. The model is completed by the imposition of an initial condition on $f(a, s, t)$ at $t = t_0$ for $s > s_0$.

Chapter 4

Numerical Techniques used

4 .1. The Semi – Lagrange Method

We consider the one-dimensional advection equation

$$\frac{\partial u}{\partial t} + c(x,t)\frac{\partial u}{\partial x} = 0$$

for $t > t$, $-\infty < x < \infty$, where u is the quantity being transported and $c(x,t)$ is the advection velocity .

The above equation, using the Lagrangian derivative

$$\frac{D}{Dt} = \frac{\partial}{\partial t} + c(x,t)\frac{\partial}{\partial x}$$

can be written as

$$\frac{Du}{Dt} = 0 \qquad \textbf{(4.1)}$$

that is, u is constant along the Lagrangian trajectory. If x is the position of the fluid quantity at time t , its trajectory is given by the equation :

$$\frac{dx}{dt} = c(x,t) \qquad \textbf{(4.2)}$$

We now consider u(x,t) to be the solution of **(4.1)** and construct a mesh with uniform space and time intervals Δx and Δt , where $x_j = j\Delta x \quad j = 0$,1,2….

and $t_n = n\Delta t \quad n$ =0,1,2,….

If u(x,t) is known at time level t_n , we can find the value of u at time level t_{n+1} , using discretization of **(4.1)** ,

$$\frac{u(x_j, t_{n+1}) - u(x_d, t_n)}{\Delta t} = 0 \ ,$$

so at time level t_{n+1} the value of $u(x_j, t_{n+1})$ is given by :

$$u(x_j, t_{n+1}) = u(x_d, t_n) \quad \textbf{(4.3)}$$

where x_d is the departure point at time level t_n of the trajectory which passes through the point (x_j, t_{n+1}). The equation **(4.3)** states that the value of $u(x_j, t_{n+1})$ is exactly equal to the value of u at the previous time level t_n. At $x = x_d$, we discretise equation **(4.1)** which expresses similar behaviour of the values of u (u does not change with time). In order to find $u(x_j, t_{n+1})$ in terms of x_d at time level t_n , we can use Euler integration method in the trajectory equation **(4.2)** and obtain :

$$\frac{(x_j, t_{n+1}) - (x_d, t_n)}{\Delta t} = c(x_j, t_n)$$

or

$$(x_d, t_n) = (x_j, t_{n+1}) - \Delta t c(x_j, t_n)$$

The departure point x_d will not necessarily coincide with a point on the grid , so we use interpolation to evaluate $u(x_d, t_n)$ [18] .

4 .2 Linear interpolation

We shall use linear interpolation in order to approximate unknown values of a function f that lie between known values of the function . So if we know the values $(x_1, f(x_1))$ and $(x_2, f(x_2))$ of a function f , the value of f at $x = x_d$ where $x_1 < x_d < x_2$ is approximated by the formula:

$$f(x_d) = f(x_1) + \frac{x_d - x_1}{x_2 - x_1}(f(x_2) - f(x_1))$$

The error in this approximation is $e = f(x) - f(x_d)$.

If f has two continuous derivatives we can prove, using Rolle's theorem, that the error e is bounded by:

$$|e| \leq \frac{(x_2 - x_1)^2}{8} \max_{x_d \in [x_1, x_2]} |f''(x_d)| \qquad [19] .$$

4 .3 Runge – Kutta Methods

Rather than use the Euler method to approximate the trajectory equation (**4.2**) we shall use a Runge - Kutta method.

Runge – Kutta methods are one-step explicit schemes and they are of the form :

$$y_{n+1} - y_n = h\phi(x_n, y_n, h)$$

where $\phi(x_n, y_n, h)$ is an approximation to

$$\int_0^1 f(y(t_n + sh), t_n + sh)ds$$

The general form of the r – stage Runge – Kutta method is defined by :

$$y_{n+1} - y_n = h\phi(x_n, y_n, h) \qquad \text{where}$$

$$\phi(x, y, h) = \sum_{i=1}^{r} c_i K_i \qquad \textbf{(4.4)}$$

$$K_1 = f(x, y) = f \qquad \textbf{(4.5)}$$

$$K_2 = f(x + ha_1, y + hb_{21}K_1) \qquad \textbf{(4.6)}$$

$$\vdots$$

$$K_i = f(x + ha_i, y + h\sum_{s=1}^{i-1} b_{is}K_s) \qquad i = 2,3,\ldots\ldots \text{r}$$

where $a_i = \sum_{s=1}^{i-1} b_{is} \qquad i = 2,3,\ldots\ldots..,r$

If we expand $\phi(x, y, h)$ in Taylor series we obtain :

$$\phi(x, y, h) = f + \frac{1}{2!}h(f_x + ff_y) + \frac{1}{3!}h^2((f_x + ff_y)f_y + f_{xx} + 2f_{xy} + f^2 f_{yy}) + O(h^3) \qquad \textbf{(4.7)}$$

Expanding the equation **(4.6)** in Taylor series we have :

$$K_2 = f + hb_{21}(f_x + K_1 f_y) + \frac{1}{2}h^2 b_{21}^2 (f_{xx} + 2K_1 f_{xy} + K_1^2 f_{yy}) + O(h^3)$$

and substituting $K_1 = f(x,y) = f$ and $a_2 = b_{21}$ we obtain :

$$K_2 = f + ha_2(f_x + ff_y) + \frac{1}{2}h^2 a_2^2 (f_{xx} + 2ff_{xy} + f^2 f_{yy}) + O(h^3)$$

Substituting in **(4.4)** we find :

$$\phi(x,y,h) = c_1 K_1 + c_2 K_2 =$$

$$c_1 f + c_2 f + c_2 ha_2(f_x + ff_y) + \frac{1}{2}h^2 a_2^2 c_2 (f_{xx} + 2ff_{xy} + f^2 f_{yy}) + O(h^3) =$$

$$(c_1 + c_2) f + hc_2 a_2 (f_x + ff_y) + \frac{1}{2}h^2 a_2 c_2 (f_{xx} + 2f_{xy} + f^2 f_{yy}) + O(h^3) \quad \textbf{(4.8)}$$

Now we compare with **(4.7)** and we have :

a) for $r = 1$ $c_2 = 0$ and so **(4.8)** gives

$$\phi(x,y,h) = c_1 f + O(h^3)$$

which is the Euler method and has order one .

b) for $r = 2$ we compare with **(4.7)** and we can find that the equations

$$c_1 + c_2 = 1 \quad \text{and} \quad c_2 a_2 = \frac{1}{2}$$

must be satisfied. These equations have a particular solution:

$$c_1 = \frac{1}{2} \ , \quad c_2 = \frac{1}{2} \ , \text{ and } \quad a_2 = 1$$

and the method in this case becomes of the form:

$$y_{n+1} - y_n = \frac{1}{2} h[f(x_n, y_n) + f(x_n + h, y_n + hf(x_n, y_n)]$$

which is known as improved Euler [20] .

This is the method that we used to calculate the numerical solution in the second step of the program .

4 .4 Trapezoidal Rule

In order to approximate equation (**3.3**) we shall need numerical integration, which is have based on the Trapezium rule.

This is a numerical method that calculates the area under a curve $y = f(x)$, using a series of trapezoids that lie in the intervals

$$[x_{j-1}, x_j] \ , \quad j = 1 \ , 2 \ , 3, \ldots\ldots \text{m}$$

We consider the function $f(x)$ over the interval [a , b] which is divided into m subintervals $[x_{j-1}, x_j]$, $j = 1 \ , 2 \ , 3, \ldots\ldots$m of width :

$$h = \frac{b - a}{m}$$

where $x_0 = a$, $x_j = x_0 + jh$ for $j = 1 \ , 2 \ , \ldots$.m-1 and $x_m = b$. The formula for the numerical approximation of the integral of $f(x)$ over [a , b] is given by:

$$\int_a^b f(x)dx = \frac{h}{2}(f(a) + f(b)) + h\sum_{j=1}^{m-1} f(x_j) + e(f,h)$$

If $f(x)$ has two continuous derivatives in [a , b], there exists value c that belongs into interval [a , b] and the error $e(f,h)$ is of the form :

$$e(f,h) = -\frac{(b-a)f''(c)}{12}h^2 \qquad [21].$$

Trapezoidal rule can be used to approximate double integrals of the form

$\int_c^d \int_a^b f(x,y)dxdy$, (see (**3.3**)) and the formula is :

$$\int_c^d \int_a^b f(x,y)dxdy = \frac{h_1}{2}\{\frac{h_2}{2}[f(a,c) + f(b,c) + 2\sum_{i=1}^{m-1} f(x_i,c)] +$$

$$\frac{h_2}{2}[f(a,d) + f(b,d) + 2\sum_{i=1}^{m-1} f(x_i,d)] +$$

$$2\sum_{j=1}^{m-1}\{\frac{h_2}{2}[f(a,y_j) + f(b,y_j) + 2\sum_{i=1}^{m-1} f(x_i,y_j)]\}\}$$

where $h_1 = \frac{d-c}{m}$ and $h_2 = \frac{b-a}{m}$ [22] .

The error using Taylor series is:

$$e(f,h_1,h_2) = O(h_1^2 h_2^2) .$$

Chapter 5

Method of solution

This model has been solved combining these numerical techniques. Equation **(3.2)** can be written as

$$\frac{\partial}{\partial t} f(a,s,t) + \frac{\partial}{\partial s}[\frac{Ra}{\Omega} f(a,s,t)] =$$

$$\dot{N}(t)\frac{a^{2i+2}}{m_{2i+2}(t)}[-f(a,s,t) + \frac{1}{(1-\lambda)^{2i+3}} f(\frac{a}{1-\lambda}, s, t)],$$

$$\text{for} \quad t > t_0 \ , \ \ s > s_0 \, .$$

Since $\frac{Ra}{\Omega} > 0$, to be well-posed it needs an initial condition and a boundary condition at $s = s_0$ (see figures A , B).

In terms of the Lagrangian derivative

$$\frac{D}{Dt} = \frac{\partial}{\partial t} + \frac{Ra}{\Omega}\frac{\partial}{\partial s}$$ the above equation becomes

$$\frac{Df(a,s,t)}{Dt} = \dot{N}(t)\frac{a^{2i+2}}{m_{2i+2}(t)}[-f(a,s,t) + \frac{1}{(1-\lambda)^{2i+3}} f(\frac{a}{1-\lambda}, s, t)] \quad (\mathbf{5.1})$$

For each a this is an inhomogeneous ordinary differential equation along a trajectory (or characteristic). To be well – posed, it needs the boundary condition expressed by **(3.4)**.

The above equation is solved numerically in two steps, where the mesh is

$$s = s_0 + jds \quad , \quad t = t_0 + ndt$$

Since $$\frac{Df(a,s,t)}{Dt} = \frac{1}{\Delta t}[f(a,s_j,t^{n+1}) - f(a,s_d,t^n)]$$

in the first step we interpolate $f(a,s,t^n)$ to get $f(a,s_d,t^n)$, i.e.

$$f(a,s,t^{n+1}) = f(a,s_d,t^n),$$

and in the second step we solve the ordinary differential equation (**5.1**) along the trajectory from d to s_j using a Runge – Kutta second order method .

The initial data function is taken to be of the form of a Gaussian hump:

$$f(a,s,t_0) = \exp[-\frac{(s-s_1)^2}{\sigma_s^2} - \frac{(a-a_1)^2}{\sigma_a^2}] \quad (\mathbf{5.1a})$$

at the point (a_1, s_1). If the trajectory intersects the boundary $s = s_0$ before reaching the line $t = t_n$ (see figures A, B) the departure point (s_0, t_d) lies on $s = s_0$ and we need the boundary condition on $s = s_0$.

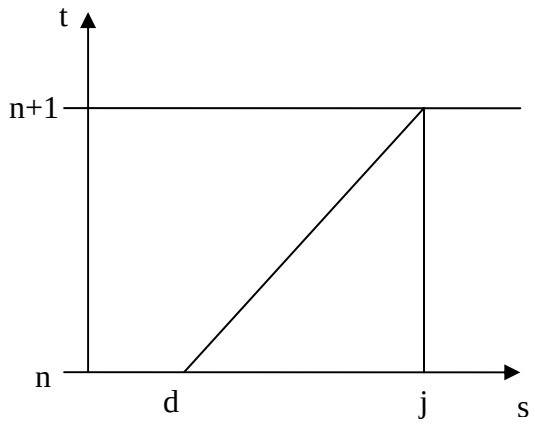

figure A

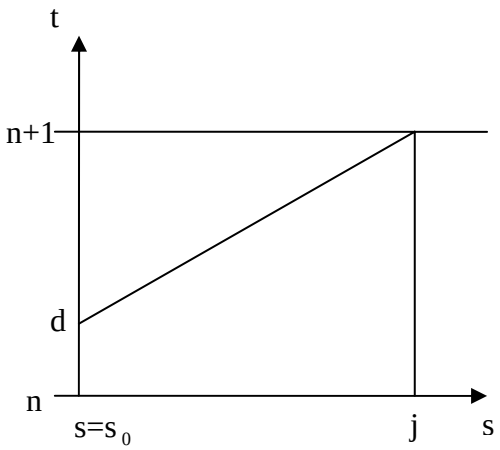

figure B

5.1 Boundary condition equation

The equation **(3.4)**, which determines the boundary condition of the model, is solved simultaneously. For $s = s_0$ we have

$$\frac{\partial f(a, s_0, t)}{\partial t} = -\frac{Raf(a, s_0, t)}{\Omega ds}$$

i.e. $$\int \frac{df(a,s_0,t)}{f} = -\int \frac{Ra}{\Omega ds} dt$$

which gives $$\ln f(a,s_0,t) = -\frac{Ra}{\Omega ds} t \ln f_0$$

or

$$f(a,s_0,t) = f_0 e^{-\frac{Rat}{\Omega ds}}$$

where $f = f_0$ at $t = 0$, and so

$$f_n(a,s_0,t) = f_0 e^{-\frac{Rat_n}{\Omega ds}} \quad \textbf{(5.2)}$$

Therefore

$$f_{n+1}(a,s_0,t) = f_0 e^{-\frac{Rat_{n+1}}{\Omega ds}} \quad \textbf{(5.3)} \ ,$$

where ds is the step size of the s interval .
If we divide **(5.2)** , **(5.3)** we obtain :

$$f_{n+1}(a,s_0,t) = f_n(a,s_0,t) e^{-\frac{Radt}{\Omega ds}}$$

These equations give the values of $f(a,s,t)$ at $s = s_0$ for all t.

To obtain $f(a,s_j,t^{n+1})$ when the trajectory intersects the boundary $s = s_0$ we solve the ordinary differential equation:

$$\frac{Df(a,s,t)}{Dt} = \dot{N}(t) \frac{a^{2i+2}}{m_{2i+2}(t)} \frac{1}{\lambda^{2i+3}} \sum_{s>s_0} f(\frac{a}{\lambda}, s, t)$$

using interpolation of $f(a,s,t)$ on the line $s = s_0$ to obtain the departure point and Runge – Kutta second order.

5.2 Normalization factor

Numerical approximation of the normalization factor

$$m_{2i+2}(t) = \int_{a_{\min}}^{a_{\max}} \int_{s_{0+1}}^{s_{\max}} a^{2i+2} f(a,s,t) ds da$$

which occurs in (**3.2**) and (**3.4**), has been calculated using a trapezoidal rule of the form:

$$\int_{a_{\min}}^{a_{\max}} \int_{s_{0+1}}^{s_{\max}} a^{2i+2} f(a,s,t) ds da = \sum_{k=0}^{m_1} \sum_{j=1}^{m} a(k)^{2i+2} da ds f(k, j)$$

where

$$m_1 = \frac{a_{\max} - a_{\min}}{da} \quad \text{and} \quad m = \frac{s_{\max} - s_0}{ds}$$

Here da and ds are step sizes of a and s respectively.

5.3 Data scaling

The given data for the equations **(3.2)** and **(3.4)** are :

$a \in [\, 10^{2}, 10^{6}\,]$, $s \in [\, 2 , 2250\,]$, $t \in [\, 10^{-7}, 10^{-1}\,]$, i = 0

N(t) = $2000\, t^{\frac{1}{3}}$, R = 1 , $\Omega = 1$ and $\lambda = 0.3$, $\lambda = 0.4$ or $\lambda = 0.5$

Because some of these numbers are quite large for the computation, we scale them as follows:

$$\hat{a} = \frac{a}{10^4} \quad , \quad \hat{s} = \frac{s}{150} \quad , \quad \hat{t} = \frac{t}{10^{-2}}$$

and so

$$\frac{\partial}{\partial s} = \frac{d\hat{s}}{ds}\frac{\partial}{\partial \hat{s}} = \frac{1}{150}\frac{\partial}{\partial \hat{s}}$$

$$\frac{\partial}{\partial t} = \frac{d\hat{t}}{dt}\frac{\partial}{\partial \hat{t}} = 10^2\frac{\partial}{\partial \hat{t}}$$

After the scaling, the equations **(3.2)** and **(3.4)** respectively become :

$$\frac{\partial}{\partial \hat{t}} f(\hat{a},\hat{s},\hat{t}) = -\frac{\partial}{\partial \hat{s}}[\frac{2R\hat{a}}{3\Omega} f(\hat{a},\hat{s},\hat{t})] +$$

$$\frac{2\hat{a}^{2i+2}}{45\hat{t}^{2/3}10^{8/3}\int_{\hat{a}_{\min}}^{\hat{a}_{\max}}\int_{\hat{s}_0}^{\hat{s}_{\max}}\hat{a}^{2i+2} f(\hat{a},\hat{s},\hat{t})d\hat{a}d\hat{s}}(-f(\hat{a},\hat{s},\hat{t}) + \frac{1}{(1-\lambda)^{2i+3}} f(\frac{\hat{a}}{1-\lambda},\hat{s},\hat{t}))$$

for $t > t_0$, $s > s_0$ and

$$\frac{\partial}{\partial \hat{t}} f(\hat{a},\hat{s}_0,\hat{t}) = -\frac{2R\hat{a}}{3\Omega d\hat{s}} f(\hat{a},\hat{s}_0,\hat{t}) +$$

$$\frac{2\hat{a}^{2i+2}}{45\hat{t}^{2/3}10^{8/3}\int_{\hat{a}_{\min}}^{\hat{a}_{\max}}\int_{\hat{s}_0}^{\hat{s}_{\max}}\hat{a}^{2i+2} f(\hat{a},\hat{s},\hat{t})d\hat{a}d\hat{s}}\frac{1}{\lambda^{2i+3}}\sum_{\hat{s}>\hat{s}_0} f(\frac{\hat{a}}{\lambda},\hat{s},\hat{t})$$

for $t > t_0$ and $s = s_0$

and the given initial data function $f(\hat{a}, \hat{s}, \hat{t}_0)$ in (**5.1a**) is :

$$f(\hat{a}, \hat{s}, \hat{t}_0) = \exp[-30^2 \frac{(\hat{s} - 1/15)^2}{100} - \frac{(\hat{a} - 90)^2}{10000}] \quad \text{at} \quad \hat{t}_0 = 10^{-5} \ .$$

Chapter 6 .

Results

We consider the following process:

At start time t_0 we deposit atoms on a thin film surface with no atoms on it, with a constant flux F. Atoms arrive on the surface, increasing its mass, and they diffuse. When atoms meet other atoms dispersing on the surface they glue together and form islands. The flux F is in inverse proportion to the diffusion so, with time, more islands are created inside smaller capture zones, the density of the islands increases, and the Voronoi polygon is updated in each time-step. If the flux is small, the deposited atoms have more time to diffuse before they meet another atom [15].

The program numerically simulates the above process.

We have plotted results of $f(a,s,t)$ against a and s after 500, 1000 and 1500 time - steps, for values of the parameter $\lambda = 0.3$, $\lambda = 0.4$ and $\lambda = 0.4$, using step sizes da=1 , ds= $2/15$ and dt=10^{-4} (see figures (**6.1**) – (**6.9**), pages 35 – 40).

There are three more graphs using step sizes da=1 , ds= $1/15$ and dt=10^{-4}, da=0.5 , ds= $2/15$ and dt=10^{-4} and da=1 , ds= $2/15$ and dt=5E-5 in the part where we have investigated the convergence of the method.

The curve moves during time to bigger values of s and smaller values of a , which is expected by the model because, with time, the fragmentation process creates more islands within smaller capture zones. (In practice this process is limited).

λ is a free parameter of the model which expresses the proportion of nucleation of new islands, and because new capture zones created (in reality)

from neighbouring island capture zones, this multiple fragmentation is linked in size with the approximation of the Voronoi polygons [23] .

J. Blackman and P. Mulheran in their later paper *" Growth of clusters on Surfaces : Monte Carlo simulations and scaling properties"* characterise the nature of the fragmentation model as crude, because it ignores the complex geometry of the Voronoi polygons network but on the other hand, the model satisfies experimental results [23] (page 201).

According to Mulheran, if we enlarge a part of the Voronoi polygon net at time-step K by a factor, we obtain the Voronoi polygon net at time-step $K-1$. This self-affine fractal behaviour of the Voronoi net is not visible on the graphs.

6.1 Convergence

If f denotes the values of the function $f(a,s,t)$ at final time t using step sizes da , ds , dt for a, s and t respectively, f_1 denotes values of the function $f(a,s,t)$ at the same time using step sizes da , $\frac{ds}{2}$, dt, f_2 the same values using step sizes da , ds, $\frac{dt}{2}$, and f_3 using step sizes $\frac{da}{2}$, ds , dt then the relative error in every case is given by the formula:

$$e_s = \frac{\sqrt{\sum_{k=0}^{m_1}\sum_{j=0}^{m}(f(k,j)-f_1(k,j))^2}}{\sqrt{\sum_{k=0}^{m_1}\sum_{j=0}^{m}(f_1(k,j))^2}}$$

$$e_t = \frac{\sqrt{\sum_{k=0}^{m_1}\sum_{j=0}^{m}(f(k,j)-f_2(k,j))^2}}{\sqrt{\sum_{k=0}^{m_1}\sum_{j=0}^{m}(f_2(k,j))^2}}$$

and

$$e_a = \frac{\sqrt{\sum_{k=0}^{m_1}\sum_{j=0}^{m}(f(k,j) - f_3(k,j))^2}}{\sqrt{\sum_{k=0}^{m_1}\sum_{j=0}^{m}(f_3(k,j))^2}}$$

where $m_1 = \frac{a_{\max} - a_{\min}}{da}$ and $m = \frac{s_{\max} - s_0}{ds}$

The figures (**6.10**), (**6.11**), and (**6.12**) are the corresponding graphs for λ=0.5 at final time $t = 0.05$ and the values of the relative errors are:

$$e_s = 0.15894, \quad e_t = 0.00745 \quad \text{and} \quad e_a = 0.117686$$

6.2 Conservation Laws

According to the model, three conservation laws should be satisfied.

i) $\int_{s_0}^{s_{\max}}\int_{a_{\min}}^{a_{\max}} af(a,s,t)dads$ expresses the total volume under the curve f and should be a constant during the fragmentation process. So the first conservation law is described by the equation

$$\int_{s_0}^{s_{\max}}\int_{a_{\min}}^{a_{\max}} af(a,s,t)dads = \Omega$$

which signifies the invariability of the volume. Initially

$$\int_{s_0}^{s_{\max}}\int_{a_{\min}}^{a_{\max}} af(a,s,t)dads = 2.806384\text{E+}14$$

which is incompatible with data but we can multiply initial data by a factor so that it is satisfied.

In the figure (**6.13**) we show an approximation of the volume conservation law for the appropriate value of Ω. The curve varies (due to numerical approximation) but only by $\frac{0.022}{2.806}$<1%.

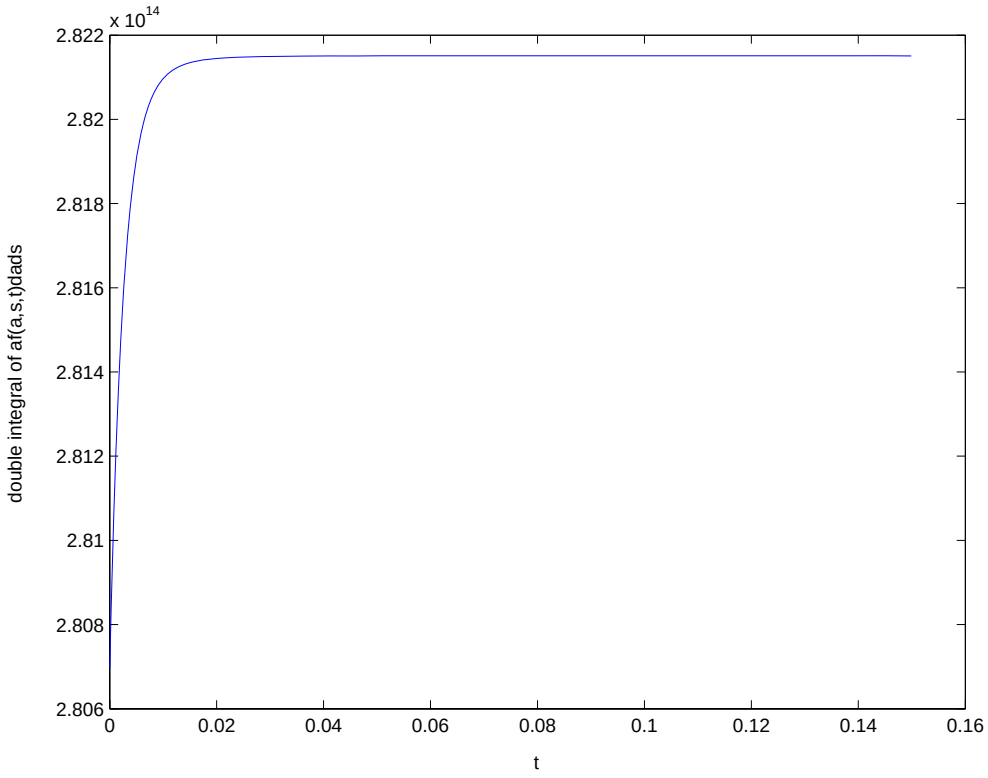

figure 6.13

$\int_{s_0}^{s_{\max}} \int_{a_{\min}}^{a_{\max}} af(a,s,t)dads$ against time after 1500time-steps (at final time=0.15).

ii) The quantity

$$\int_{s_0}^{s_{\max}} \int_{a_{\min}}^{a_{\max}} sf(a,s,t)dads$$

expresses the total mass of the system deposited and, according to the model, increases linearly with time. So the second conservation law is

$$\int_{s_0}^{s_{\max}} \int_{a_{\min}}^{a_{\max}} sf(a,s,t)dads = \mathrm{R}\,t$$

Similarly we observe that the given initial data function is not satisfied initially for $t = t_0 = 10^{-5}$ and $R = 1$ because

$$\int_{s_0}^{s_{\max}} \int_{a_{\min}}^{a_{\max}} sf(a,s,t_0)dads = 13807307312.3 \neq Rt_0$$

In figure (**6.14**) we can see an approximation to the second conservation law for appropriate values of R , t and initial data function.

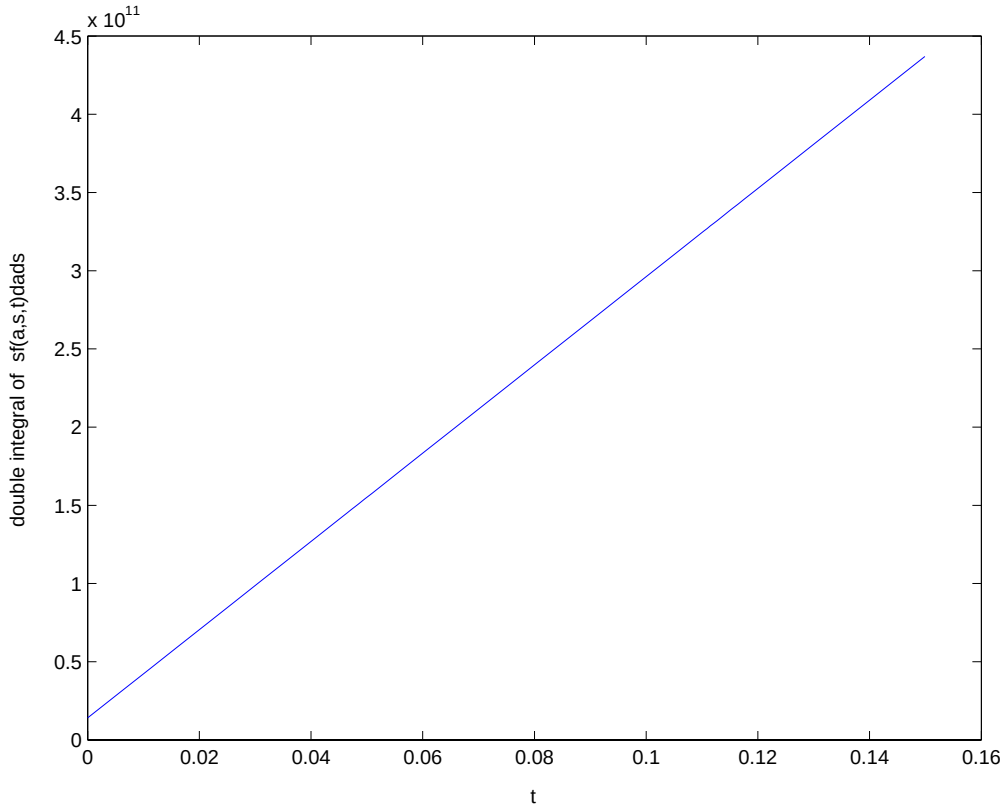

figure 6.14

$\int_{s_0}^{s_{\max}} \int_{a_{\min}}^{a_{\max}} sf(a,s,t)dads$ against time after 1500time-steps (at final time=0.15).

We observe that the curve is linear but the scale is wrong.

iii) The third conservation law, which expresses the total number of islands, is:

$$\int_{s_0}^{s_{\max}} \int_{a_{\min}}^{a_{\max}} f(a,s,t)\,da\,ds = N(t) \quad (\mathbf{6.1})$$

where $N(t)$ denotes the number of islands at time t

and is also not satisfied by the given initial data function because:

a) at $t = t_0 = 10^{-5}$ the left hand side of the equation (**6.1**) gives

$$\int_{s_0}^{s_{\max}} \int_{a_{\min}}^{a_{\max}} f(a,s,t_0)\,da\,ds = 503305041.195$$

and the right hand side $N(t_0) = 9.28317618081$

b) the graph of $\int_{s_0}^{s_{\max}} \int_{a_{\min}}^{a_{\max}} f(a,s,t)\,da\,ds$ is a "straight line" (up to 2% error) figure (**6.15**), while the graph of the function $N(t)$ increases with time figure (**6.16**). We do not have a reason for this behaviour.

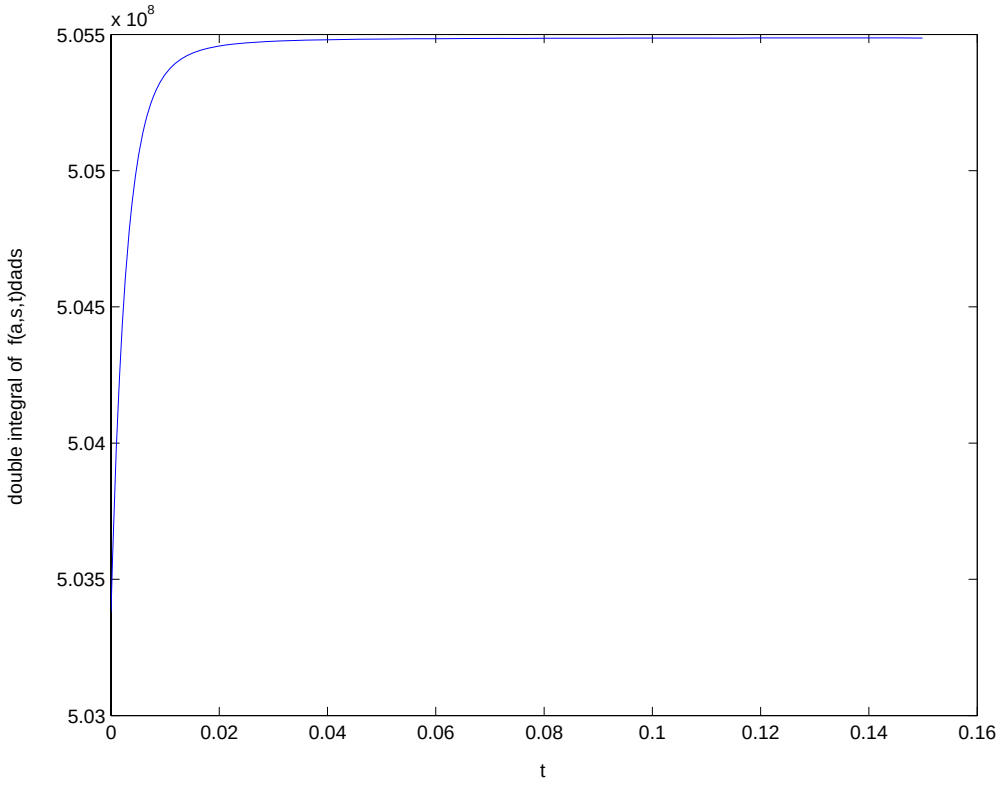

figure 6.15

$\int_{s_0}^{s_{\max}} \int_{a_{\min}}^{a_{\max}} f(a,s,t)dads$ against time after 1500time-steps (at final time=0.15).

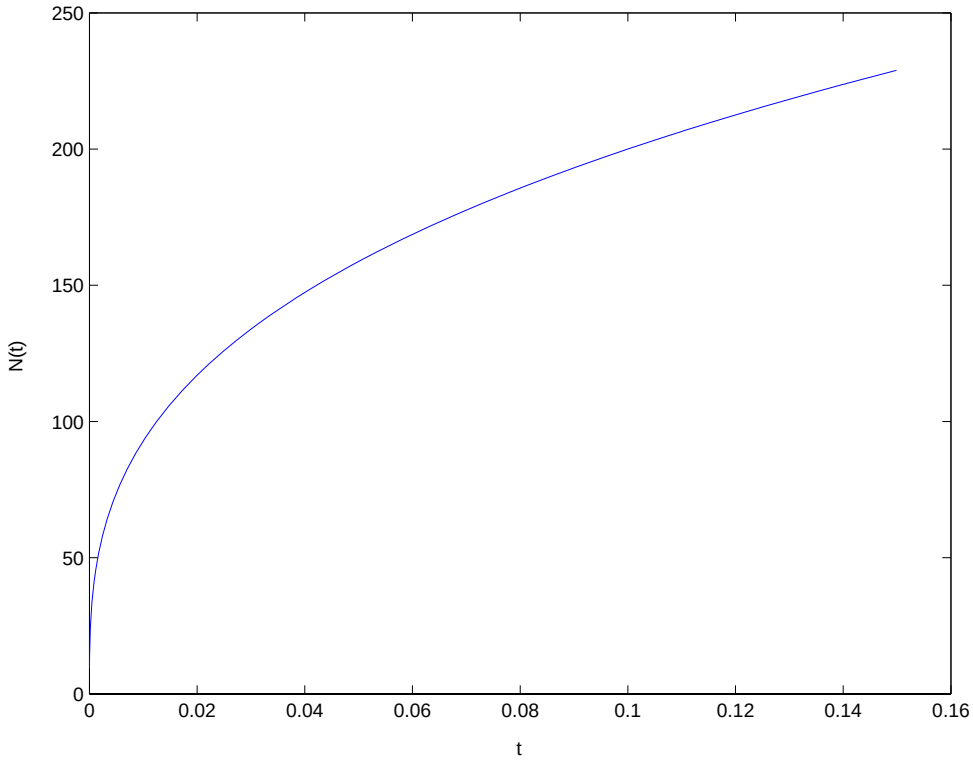

figure 6.16

N(t) against time after 1500time-steps (at final time=0.15).

Chapter 7

Discussion

The *" Theory of the island and capture zone size distributions in thin film growth"* is based on a brilliant study *"Fractal concepts in surface growth"* by A.L. Barabasi and H. E. Stanley [15], and experimental results in film deposition by P. Mulheran and J. Blackman (Phys. Rev B, 53 (1996) 10261).

The boundary condition equation (**3.4**) contains the term ds, step –size in s direction according to the model, which is finite in the equation but it becomes an infinitesimal quantity during the process of the numerical solution. The term belongs to the denominator so for very small values of ds, which give better approximation to the numerical method, may produce problems in the model's stability .

The numerical methods we used at first in this project were splitting with First Order Upwind and Euler, but the results were not satisfactory because of the first order accuracy of the methods. The second order combination of semi-Lagrange and Runge-Kutta proved more satisfactory. All methods contain a time consuming loop which approximates the value of $m_{2i+2}(t)$, in which $f(a,s,t)$ is involved, in two places in the programme for K_2 calculation (equations **3.2** and **3.4**). The programme, which runs for small values of da and ds on the limits of the computer, using step sizes da=1 , ds=$2/15$ and dt=10^{-4} for a, s, t respectively, needs 80 minutes to produce results at final time t=0.15 .

This project, unfortunately, finishes with a discrepancy in the paragraph where we discussed the conservation laws to be satisfied, but we ran out of time.

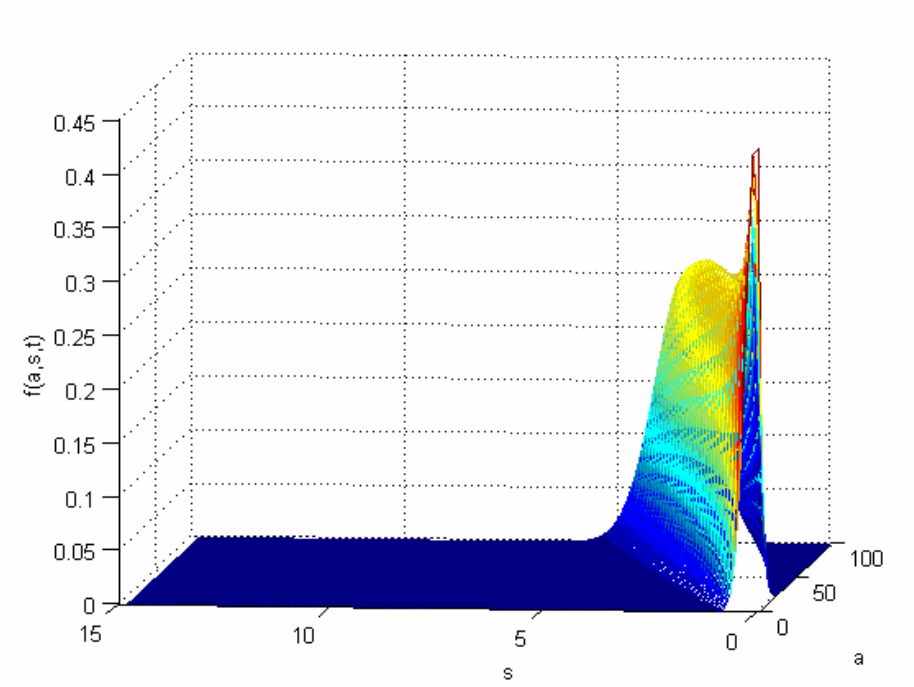

figure 6.1

f(a,s,t) for λ =0.3 after 500 time-steps (final time =0.05).

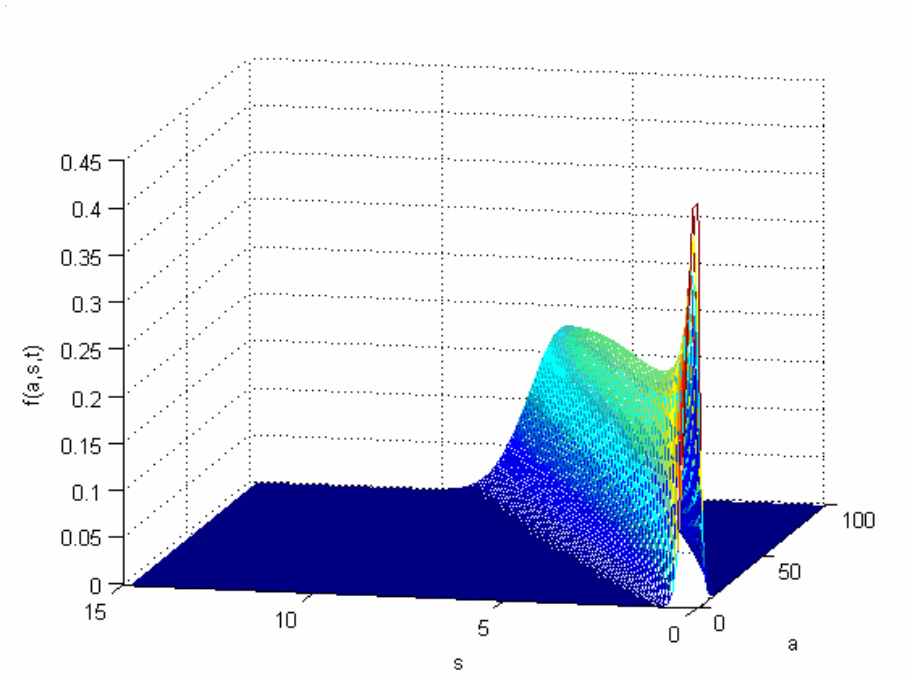

figure 6.2

f(a,s,t) for λ =0.3 after 1000 time-steps (final time = 0.1).

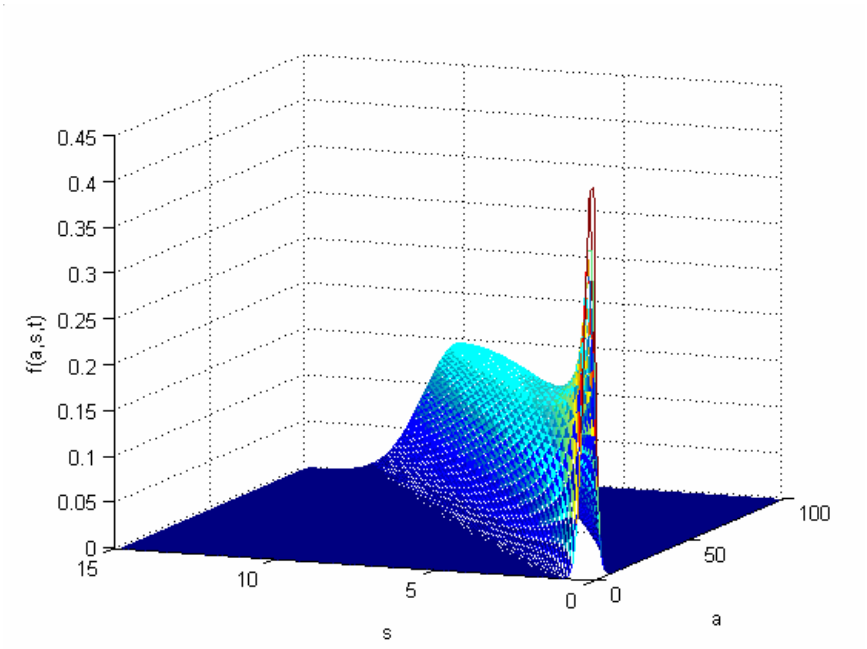

figure 6.3

f(a,s,t) for λ =0.3 after 1500 time-steps (final time =0.15).

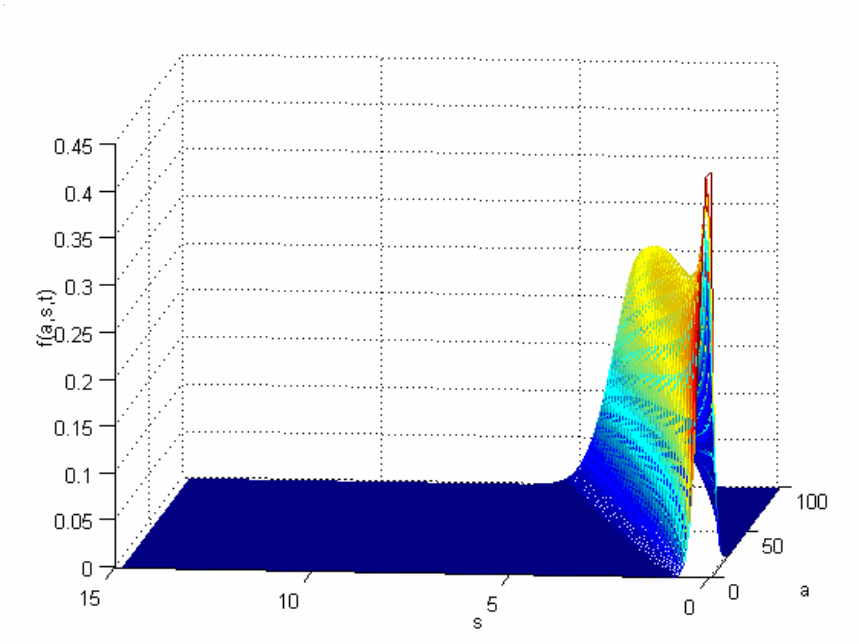

figure 6.4

f(a,s,t) for λ =0.4 after 500 time-steps (final time =0.05).

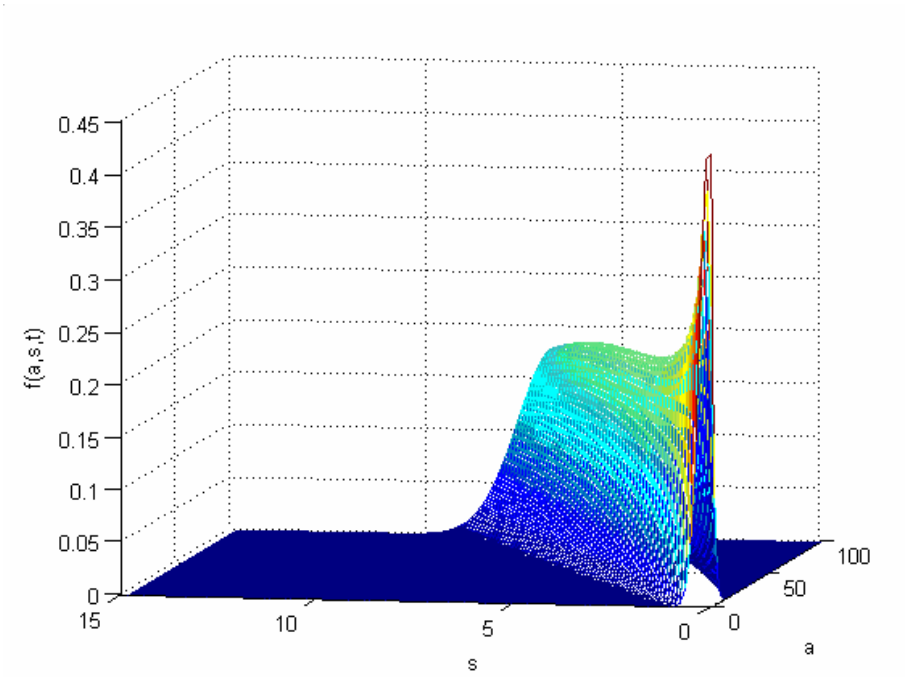

figure 6.5

f(a,s,t) for λ =0.4 after 1000 time-steps (final time =0.1).

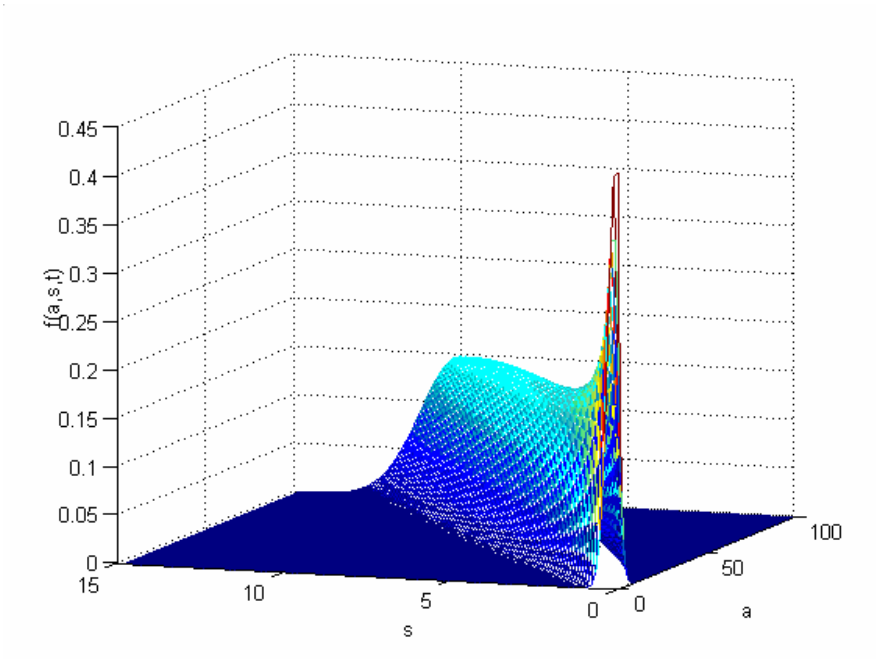

figure 6.6

f(a,s,t) for λ =0.4 after 1500 time-steps (final time =0.15).

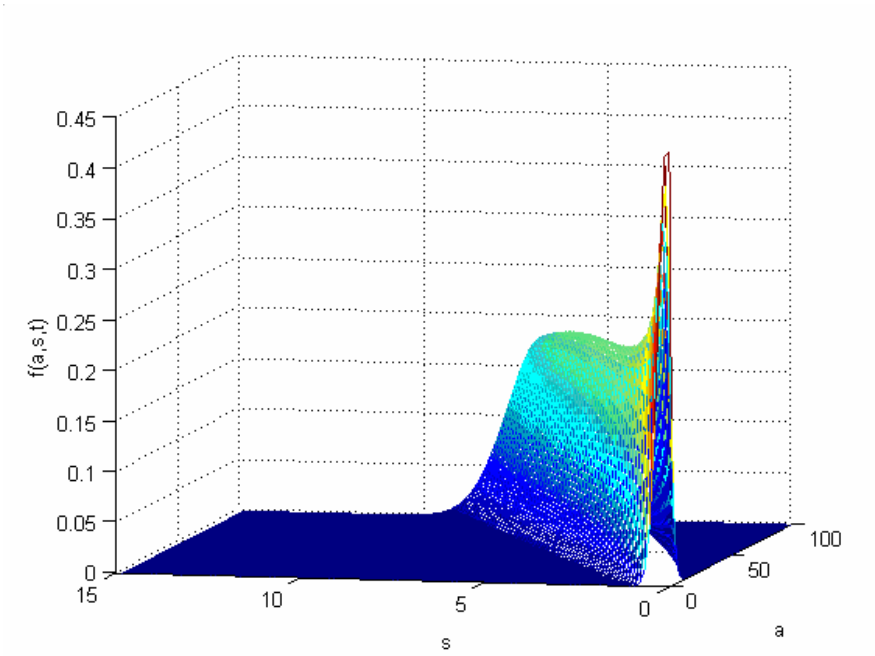

figure 6.7

f(a,s,t) for λ =0.5 after 1000 time-steps (final time =0.1).

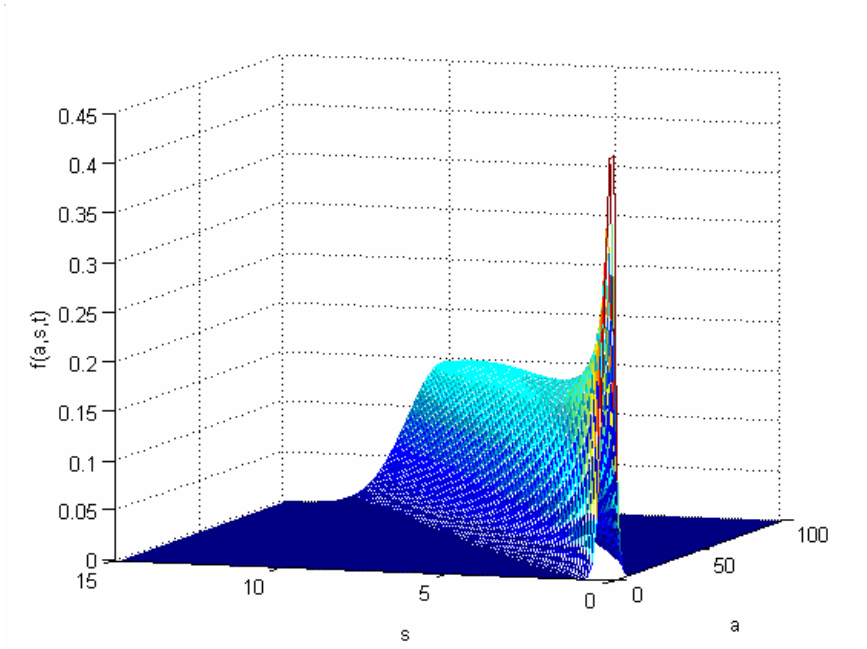

figure 6.8

f(a,s,t) for λ =0.5 after 1500 time-steps (final time =0.15).

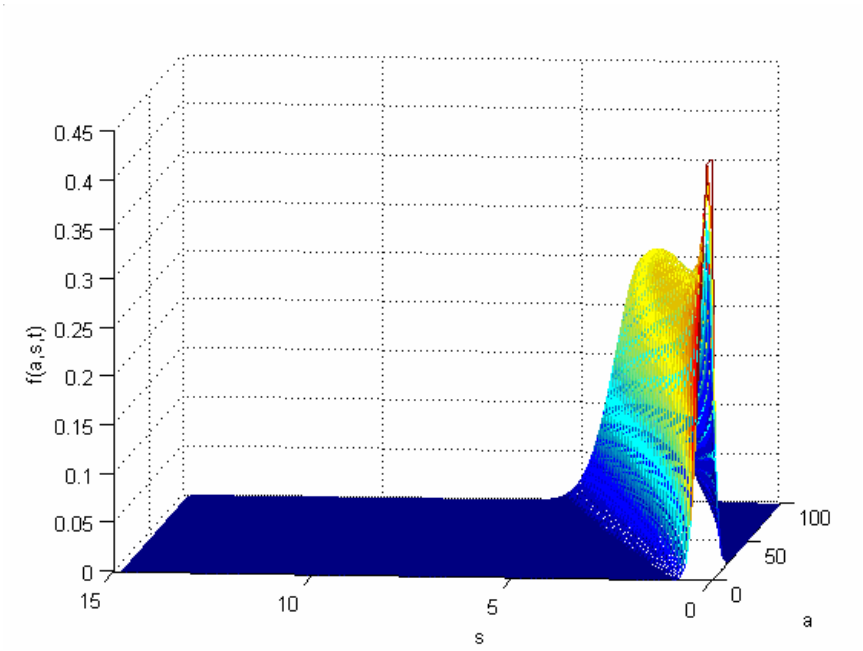

figure 6.9

f(a,s,t) for λ =0.5 after 500 time-steps (final time =0.05).

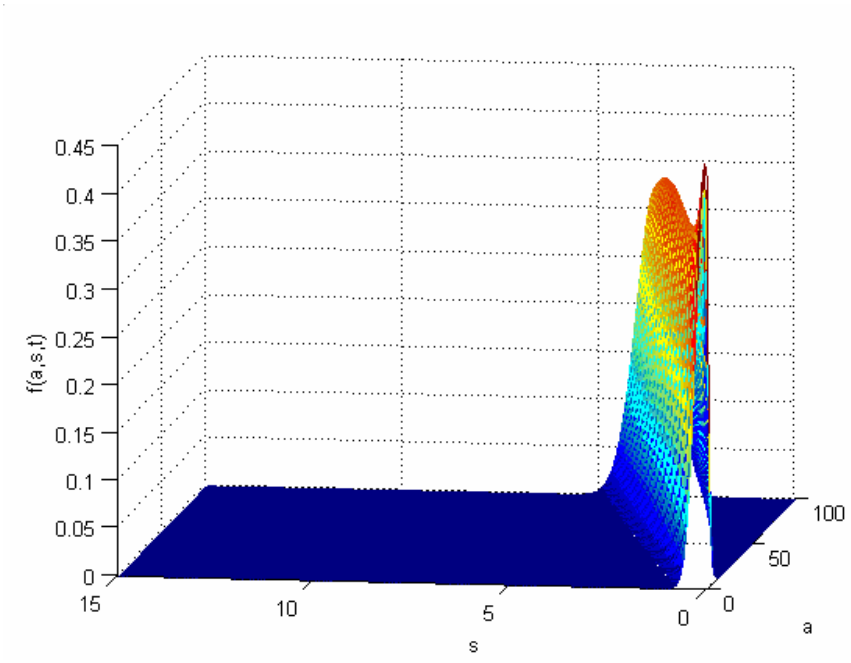

figure 6.10

f(a,s,t) for λ =0.5 and ds= $1/15$ after 500 time-steps (final time =0.05).

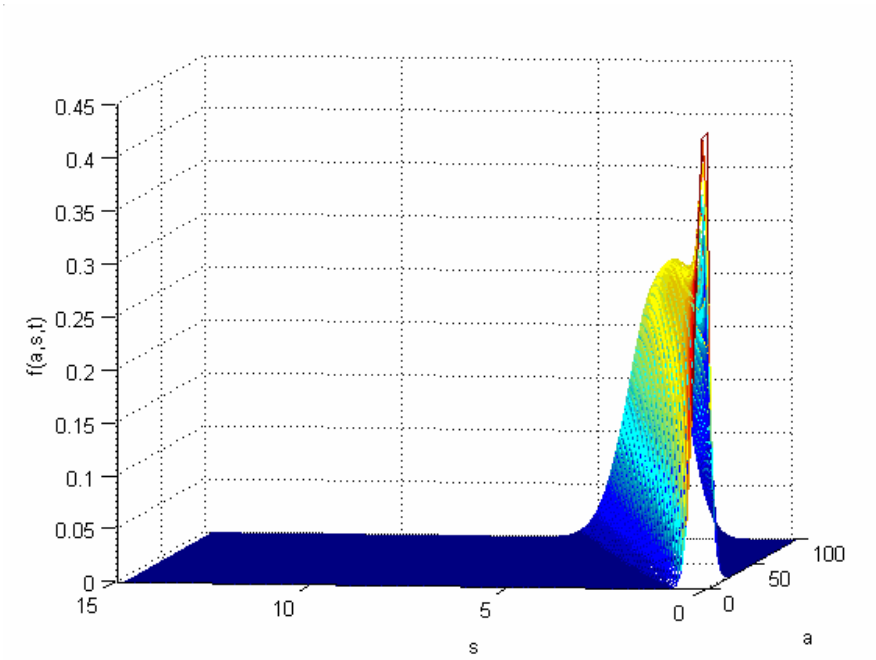

figure 6.11

f(a,s,t) for λ =0.5 and dt=5E-5 after 500 time-steps (final time =0.05).

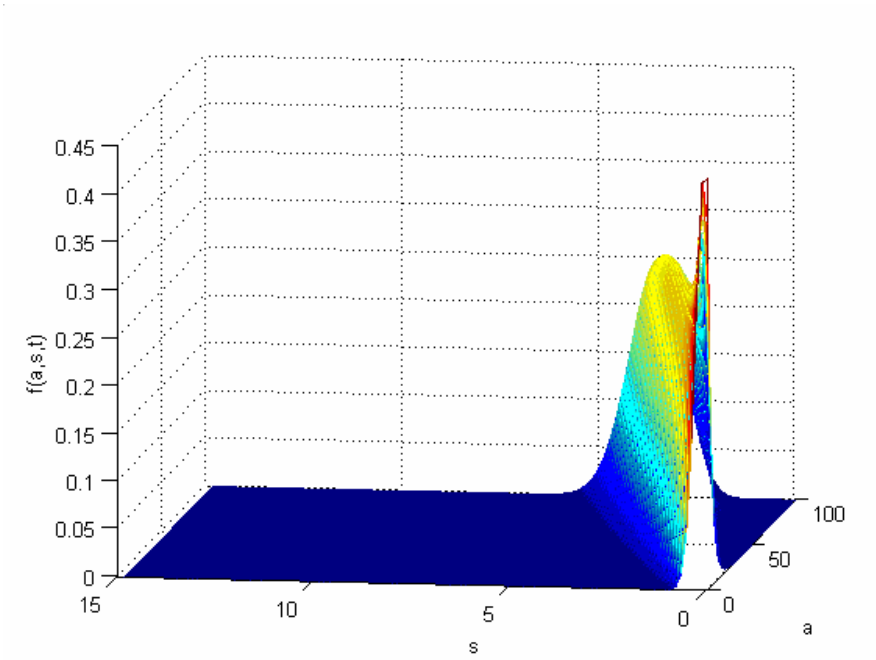

figure 6.12

f(a,s,t) for λ =0.5 and da=0.5 after 500 time-steps (final time =0.05).

Bibliography

[1] John Pickrell, http://www.newscientist.com/popuparticle.ns?id=in64, viewed 1/7/2005 .

[2] http://en.wikipedia.org/wiki/Nanotechnology , viewed 2/7/2005 .

[3] Rachel Nowak, http://www.newscientist.com/article.ns?id=dn6841&print=true, viewed 2/7/2005 .

[4] Stephen Wood, Richard Jones and Alison Geldart, http://www.azonano.com/details.asp?ArticleID=1207#_Length _Scales_for_Nanomaterials%20(Me , viewed 2/7/2005 .

[5] Microgravity News staff at Hampton University (winter 2000) http://spaceresearch.nasa.gov/general_info/nanosciense_lite.html , viewed 1/7/2005 .

[6] Natasha Loder The Economist (1/1/2005): *"Small Wonders A survey of Nanotechnology"* .

[7] R. P. Raffaelle, S. L. Castro, A. F. Hepp, and S. G. Bailey , http://www.grc.nasa.gov/WWW/RT2001/5000/5410bailey1.html , viewed 30/7/2005 .

[8] C. Brahic and M. Shanahan, http://www.azonano.com/details.asp?ArticleID=1134#_What_is_ Nanotechnology? , viewed 2/7/2005 .

[9] http://www.azonano.com/details.asp?ArticleID=449 , viewed 2/7/2005 .

[10] http://en.wikipedia.org/wiki/Nanomedicine , viewed 15/7/2005 .

[11] Robert A. Freitas Jr. , http://www.rfreitas.com/Nano/FutureNanofabNMed.htm , viewed 15/7/2005.

[12] http://www.answers.com/grey%20goo , viewed 26/7/2005 .

[13] http://www.greenpeace.org.uk/contentlookup.cfm?ucidparam =20031003120335&Me... , viewed 26/7/2005 .

[14] Andrew Zangwill http://www.nature.com/materials/news/newsandviews /010607/journal/411651a0.html, viewed 31/7/2005 .

[15] A.-L. Barabasi, H. E. Stanley (1995), *Fractal concepts in surface growth.* Cambridge University Press.

[16] P.A. Mulheran , J . A . Blackman (1996), *Capture zones and scaling in homogeneous thin- film growth* . Physical review B Volume 53, number 15 pages 10261 – 10267.

[17] P. A. Mulheran, D. A. Robbie (2000), *Theory of the island and capture zone size distribution in thin film growth.* Europhysics Letters 49 (5), pages 617-623.

[18] C.J. Smith (1993), *Error measurements for Semi-Lagrangian Schemes* . Numerical Analysis report 3/93.Department of Mathematics, University of Reading.

[19] http://en.wikipedia.org/wiki/Linear_interpolation , viewed 27/7/2005 .

[20] J.D. Lambert, (1973), *Computational methods in ordinary differential equations* . Chichester; London: Wiley.

[21] http://math.fullerton.edu/mathews/n2003/TrapezoidalRuleMod.html , viewed 27/7/05.

[22] D. Keffer, http://clausius.engr.utk.edu/che301/pdf/exam_f99s_04.pdf , viewed 24/7/2005.

[23] J.A. Blackman , P.A. Mulheran (2001), *Growth of clusters on surfaces: Monte Carlo simulations and scaling properties*. Computer Physics Communications 137 pages 195-205.